Statistical analysis of cogging torque considering various manufacturing imperfections (repository copy)

Article:

Gerber, S. and Wang, R-J., (2016) Statistical analysis of cogging torque considering various manufacturing imperfections, *Proc. of XXII International Conference on Electrical Machines*, (ICEM), pp. 2066--2072, Lausanne, Switzerland, 4-7 Sept. 2016.

http://dx.doi.org/10.1109/ICELMACH.2016.7732807

Statistical Analysis of Cogging Torque Considering Various Manufacturing Imperfections

Stiaan Gerber, *Member, IEEE* and Rong-Jie Wang, *Senior Member, IEEE*

***Abstract*—Cogging torque in permanent magnet machines is undesirable because it is a source of noise and vibration and because it has a negative impact on controllability. Over the years, many design techniques that can effectively reduce cogging torque have been developed. However, due to manufacturing tolerances, a machine's cogging torque characteristics often deviate from that intended with the design. In this paper, an analytical model of cogging torque in permanent magnet machines with surface-mounted magnets is developed. The model is capable of accounting for various manufacturing imperfections that can have an impact on cogging torque. The low computational complexity of the model allows statistical analyses of the cogging torque to be conducted using Monte Carlo simulations. Using this approach, it is possible to obtain the probability density distribution of the cogging torque, given the error distributions of critical machine features.**

***Index Terms*—analytical models, cogging torque, computational complexity, Monte Carlo methods, mass production, permanent magnet machines**

I. Nomenclature

p	Number of pole pairs
Q	Number of stator slots
L	Stack length
T	Torque
G	Relative permeance
B_a	Flux density at left side of slot
B_b	Flux density at right side of slot
R	Torque arm
B'	Flux density in an equivalent slotless machine
R_s	Radius of the stator surface
R_m	Radius of the magnet side facing the air-gap
R_r	Radius of the rotor yoke side facing the air-gap
α	Rotor position
θ	Tangential coordinate
ϕ	Variable of integration
β_m	Magnet pitch to pole pitch ratio
β_s	Slot opening to slot pitch ratio
h_m	Magnet height
g	Air-gap length
θ_{si}	Tangential coordinate of center of slot i
θ_{mj}	Tangential coordinate of center of magnet j
B_{anj}	Fourier coefficients for flux density of magnet j
M_{anj}	Fourier coefficients for remanence of magnet j

This work was supported by ABB Corporate Research, Sweden.

S. Gerber and R-J. Wang are with the Department of Electrical and Electronic Engineering, Stellenbosch University, Stellenbosch, South Africa (e-mail: sgerber@sun.ac.za, rwang@sun.ac.za)

II. Introduction

Cogging torque is an attribute of slotted permanent magnet (PM) machines caused by the variation of energy stored in the magnetic field of these machines as the rotor position changes. Due to the undesirable consequences of cogging torque, i.e. noise, vibration and negative impact on control precision, cogging torque in PM machines has been studied extensively [1]–[16]. A number of design techniques that can effectively reduce cogging torque have been developed, such as stator skewing, rotor skewing, magnet pole arc optimization, magnet shifting, magnet shaping, slot opening optimization, auxiliary stator teeth and pole/slot combination selection [1]–[4].

Unfortunately, cogging torque in PM machines often exhibit high sensitivity to geometrical and material parameters and thus, design efforts to reduce cogging torque can be negated to some extent by imperfections arising in the manufacturing process [5]. Recent works on cogging torque have investigated the impacts of manufacturing imperfections on cogging torque. Errors in magnet placement have been considered in [6] while the impact of magnetization faults have been studied in [7]. In [8], various imperfections of the rotor were considered in a design of experiments using finite element analysis (FEA). A detailed subdomain model of surface-mounted PM machines that can account for several manufacturing imperfections has been presented in [9].

Modeling cogging torque is challenging. While FEA can give accurate results, the computational cost is typically very high due to the fine mesh required for accuracy. Thus, analytical methods – of which several have been developed – may be preferred for their speed. These include methods based on relative air-gap permeance [10], complex permeance [11] and subdomain models [12].

In this paper, a relatively simple analytical model of cogging torque is developed that can account for imperfections that can have a significant effect on cogging torque. Since the computational complexity of the model is low, it is readily applied in statistical analyses of cogging torque using Monte Carlo simulations. Using this approach, the probability density distribution of the cogging torque of a machine can be obtained, given the probability distributions of critical machine features. This can be a powerful tool in mass production environments where it can be used to predict what percentage of machines manufactured will meet a given maximum cogging torque specification.

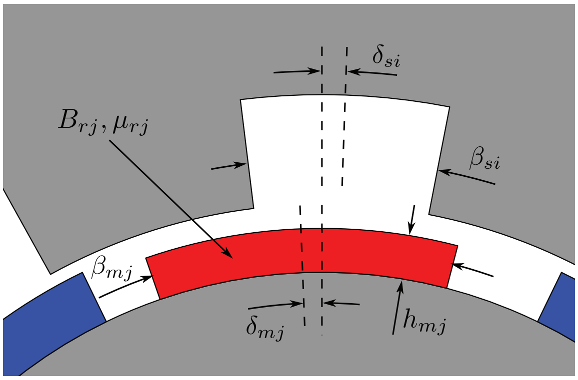

(a)

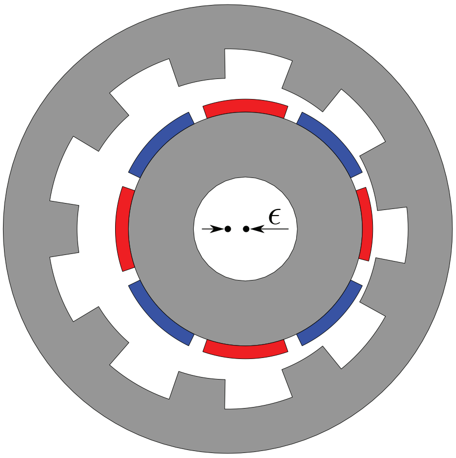

(b)

Fig. 1. Manufacturing imperfections considered in the analytical model. (a) Stator and rotor imperfections. (b) Static eccentricity.

III. Analytical Modeling of Cogging Torque Including Imperfections

For the purpose of statistical analysis, the computational cost of simulating cogging torque using the finite element method is prohibitively high. Quick analytical methods are required. In this paper, the method of integrating the net lateral force acting on slot sides [10], [13] has been adopted and extended to account for various manufacturing imperfections. The imperfections and the affected model parameters are listed in Table I and illustrated in Fig. 1. A detailed description of the method is given in this section.

TABLE I
Parameters Used to Account for Manufacturing Imperfections

Imperfection	Parameter
Variations in magnet remanence	M_{rj}
Variations in magnet recoil permeability	μ_{rj}
Variations in magnet height/thickness	R_{mj}
Variations in magnet pitch/width	β_{mj}
Variations in stator slot opening	β_{si}
Errors in the positioning of magnets	δ_{mj}
Errors in the positioning of slots	δ_{si}
Static eccentricity	ϵ

A. Basic Model

The model assumes that the flux density in the air-gap of a slotted machine can be calculated by multiplying the air-gap flux density in an equivalent slotless machine with a relative permeance function. Inside slots, it is assumed that flux lines follow circular paths, as illustrated in Fig. 2 such that the magnitude of the flux density at the slot sides is equal to that at the stator surface. The torque can then be calculated by integrating Maxwell's stress tensor on each slot side and multiplying by the torque arm:

$$T(\alpha) = \frac{L}{2\mu_0} \sum_{i=1}^{Q} \int_{\theta_0}^{\frac{\beta_{si}\pi}{Q}} G^2(\phi)\left[B_a^2(\phi,\alpha) - B_b^2(\phi,\alpha)\right] R(\phi) \mathrm{d}\phi \tag{1}$$

$$G(\phi) = \frac{\frac{h_m}{\mu_r} + g}{\frac{h_m}{\mu_r} + g + R_s(\frac{\beta_s \pi}{Q} - \phi)\frac{\pi}{2}} \tag{2}$$

$$B_a(\phi,\alpha) = B'(\theta_{si} + \phi - \alpha) \tag{3}$$

$$B_b(\phi,\alpha) = B'(\theta_{si} - \phi - \alpha) \tag{4}$$

$$R(\phi) = R_s + R_s\left(\frac{\beta_s \pi}{Q} - \phi\right) \tag{5}$$

In these equations, α is the rotor position, G is the relative permeance, B_a and B_b are the flux densities evaluated on the left and right sides of a slot respectively and R is the torque arm. B' is the flux density in an equivalent slotless machine and $\theta_{si} = \frac{2\pi i}{Q}$ represents the tangential position of slot i. For a more in depth discussion of the method, the reader is referred to [10], [13], [14].

B. Modeling of Rotor Imperfections

Variations in magnet characteristics are common in PM machines. Magnets typically differ in their geometry and

$$B_{anj} = \frac{-2\mu_0 n M_{anj}}{R_s(n^2-1)}\left(\frac{R_s}{R_{mj}}\right)^n \cdot \frac{(1-n)R_{mj} - 2R_r \left(\frac{R_r}{R_{mj}}\right)^n + (1+n)R_{mj}\left(\frac{R_r}{R_{mj}}\right)^{2n}}{(1-\mu_{rj})\left(1 - \left(\frac{R_s}{R_{mj}}\right)^{2n}\left(\frac{R_r}{R_{mj}}\right)^{2n}\right) + (1+\mu_{rj})\left(\left(\frac{R_s}{R_{mj}}\right)^{2n} - \left(\frac{R_r}{R_{mj}}\right)^{2n}\right)} \tag{6}$$

$$B_{a1j} = \frac{-\mu_0 M_{a1j} \left[\left(\frac{R_r}{R_{mj}}\right)^2 \left(2\ln\frac{R_r}{R_{mj}} + 1\right) - 1\right]}{(1-\mu_{rj})\left(1 - \left(\frac{R_s}{R_{mj}}\right)^2\left(\frac{R_r}{R_{mj}}\right)^2\right) + (1+\mu_{rj})\left(\left(\frac{R_s}{R_{mj}}\right)^2 - \left(\frac{R_r}{R_{mj}}\right)^2\right)} \tag{7}$$

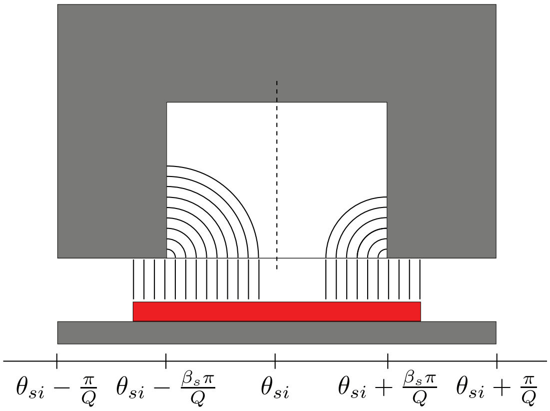

Fig. 2. Assumed flux paths inside slots, according to the model presented in [10], [13].

in magnetization characteristics. The analytical model under discussion considers five types of imperfection associated with each magnet. These are variations in remanence, recoil permeability, magnet pitch/width, magnet height and tangential magnet location. These imperfections are considered in the calculation of B'. In this model, B' is constructed by superposition of the fields produced by individual magnets,

$$B'(\theta) = \sum_{j=1}^{2p} B'_j(\theta - \theta_{mj}) \tag{8}$$

where $2p$ is the number of poles and $\theta_{mj} = \frac{\pi j}{p}$ is the nominal location of magnet j. An expression for B'_j in terms of a Fourier cosine series is obtained using a similar approach as described in [15], but only considering a single magnet.

$$B'_j(\theta) = \sum_{n=1}^{\infty} B_{anj} \cos n(\theta - \theta_{mj}) \tag{9}$$

Expressions for the coefficients B_{an} are given in (6) and (7). Variations in magnet remanence and recoil permeability are modeled by adjusting the coefficients M_{anj} and μ_{rj} for each magnet. Variations in magnet width are also reflected in M_{anj}. For radial magnetization, M_{anj} can be expressed as

$$M_{anj} = \frac{2M_{rj}}{\pi n} \sin \frac{\beta_{mj} \pi n}{2p} \tag{10}$$

Magnet heights are adjusted via R_{mj}, the radius of the magnet side facing the air-gap. Magnets are considered to lie flush with the rotor yoke, no provision for radial displacement is made. Errors in tangential magnet location are included in the model by modifying (8) to include a displacement error component,

$$B'(\theta) = \sum_{j=1}^{2p} B'_j(\theta - \theta_{mj} - \delta_{mj}) \tag{11}$$

with δ_{mj} the displacement error of magnet j.

C. Modeling of Stator Imperfections

Variations in stator slot openings are considered by modifying the expression (2) for individual slots. This is accomplished by simply substituting an appropriate value of β_s for each slot.

$$G_i(\phi) = \frac{\frac{h_m}{\mu_r} + g}{\frac{h_m}{\mu_r} + g + R_s(\frac{\beta_{si}\pi}{Q} - \phi)\frac{\pi}{2}} \tag{12}$$

Errors in slot position are handled by shifting the range over which the flux density is evaluated to coincide with the position of the stator slots. Thus, (3) and (4) become

$$B_a(\phi, \alpha) = B'(\theta_{si} - \delta_{si} + \phi - \alpha) \tag{13}$$

$$B_b(\phi, \alpha) = B'(\theta_{si} - \delta_{si} - \phi - \alpha) \tag{14}$$

with δ_{si} the tangential displacement of each slot about its nominal position.

D. Modeling of Eccentricity

The model can be further modified to account for static and dynamic eccentricity by expressing the air-gap length in terms of the tangential coordinate θ and the rotor position α. In this work, only static eccentricity is considered and the air-gap length is approximated as [16]

$$g(\theta) = g_0(1 - \epsilon)\cos\theta \tag{15}$$

with g_0 the mean air-gap length and ϵ the displacement of the rotor's axis from the stator's axis normalized relative to g_0. When eccentricity is considered, the relative permeance on the two sides of a slot are no longer equal and (1) has to be expressed as

$$T(\alpha) = \frac{L}{2\mu_0} \sum_{i=1}^{Q} \int_{\theta_0}^{\frac{\beta_{si}\pi}{Q}} \big[G_{ai}^2(\phi) B_a^2(\phi, \alpha) - G_{bi}^2(\phi) B_b^2(\phi, \alpha)\big] R(\phi) \mathrm{d}\phi \tag{16}$$

with

$$G_{ai}(\phi) = \frac{\frac{h_m}{\mu_r} + g_0}{\frac{h_m}{\mu_r} + g(\theta_{si} + \phi) + R_s(\frac{\beta_{si}\pi}{Q} - \theta)\frac{\pi}{2}} \tag{17}$$

$$G_{bi}(\phi) = \frac{\frac{h_m}{\mu_r} + g_0}{\frac{h_m}{\mu_r} + g(\theta_{si} - \phi) + R_s(\frac{\beta_{si}\pi}{Q} - \theta)\frac{\pi}{2}} \tag{18}$$

E. Model Verification

In order to assess the accuracy of the analytical model, the impact of individual imperfections on the cogging torque of two machines have been calculated using the model and FEA. Cross-sections of the machines are shown in Fig. 3 and their parameters are listed in Table II. All simulations have been conducted assuming a stack length of 1 m, giving results per unit of stack length.

The results of the comparisons are listed in Tables III and IV. Although the model does not predict the amplitude of the cogging torque with high precision, there is a similar trend in the impact of the various imperfections predicted

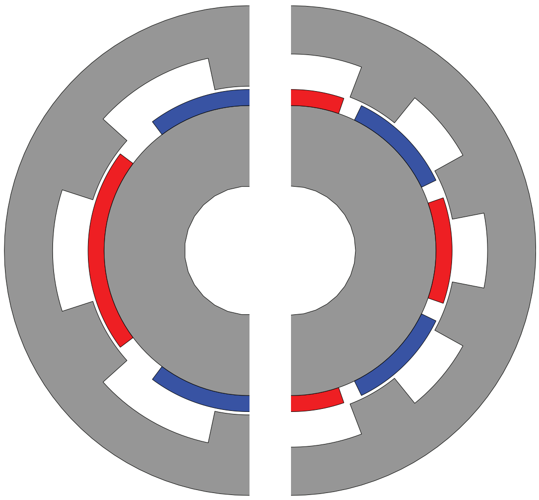

Fig. 3. Cross-sections of machines used for case studies. (a) Machine A. (b) Machine B.

TABLE II
PARAMETERS OF CASE STUDY MACHINES

Parameter	Machine A	Machine B
Pole pairs p	2	4
Stator slots Q	6	9
Outer radius R_o	76 mm	76 mm
Stator yoke height h_{sy}	15 mm	15 mm
Stator slot height h_{sl}	10 mm	10 mm
Magnet height h_m	5 mm	5 mm
Rotor yoke height h_{ry}	25 mm	25 mm
Air-gap length g_0	1 mm	1 mm
Magnet pitch β_m	0.82	0.85
Slot pitch β_s	0.6	0.55
Remanent flux density B_r	1.2	1.2
Relative recoil permeability μ_r	1.05	1.05

by the model and FEA. The cogging torque waveforms of machine B are also shown in Fig. 4. It can be seen that the shape of the waveforms calculated using the model resemble those calculated with FEA.

Although, the accuracy of the analytical model can be improved, the impact of imperfections may be modeled adequately for statistical analyses to reveal important characteristic trends in cogging torque variation.

TABLE III
COMPARISON OF MODELS CONSIDERING INDIVIDUAL IMPERFECTIONS: MACHINE A

Imperfection	Magnitude	Torque [Nm]		Impact [p.u.]	
		Model	FEM	Model	FEM
Base	n.a.	45.07	47.32	1.00	1.00
M_r	-20 %	42.58	44.73	0.94	0.95
μ_r	+20 %	41.42	46.14	0.92	0.98
h_m	-20 %	41.26	43.71	0.92	0.92
β_m	-0.1	57.11	79.25	1.27	1.67
β_s	-0.1	66.28	62.56	1.47	1.32
δ_m	5 % of $\frac{\pi}{p}$	73.63	86.57	1.63	1.83
δ_s	5 % of $\frac{2\pi}{Q}$	60.89	81.94	1.35	1.73
ϵ	0.2	45.27	47.56	1.00	1.01

TABLE IV
COMPARISON OF MODELS CONSIDERING INDIVIDUAL IMPERFECTIONS: MACHINE B

Imperfection	Magnitude	Torque [Nm]		Impact [p.u.]	
		Model	FEM	Model	FEM
Base	n.a.	1.09	1.39	1.00	1.00
M_r	-20 %	18.20	30.13	16.75	21.62
μ_r	+20 %	3.51	13.28	3.23	9.53
h_m	-20 %	17.37	32.17	15.98	23.09
β_m	-0.1	42.07	47.88	38.71	34.37
β_s	-0.1	29.13	44.92	26.80	32.25
δ_m	5 % of $\frac{\pi}{p}$	22.68	43.59	20.87	31.29
δ_s	5 % of $\frac{2\pi}{Q}$	27.10	40.33	24.94	28.95
ϵ	0.2	13.45	30.80	12.38	22.11

IV. STATISTICAL MODELING OF COGGING TORQUE

A. Overview

The analytical model presented in the previous section allows quick evaluation of cogging torque and is capable of modeling manufacturing imperfections. These capabilities make it possible to conduct statistical analyses of the cogging torque of a machine. The aim of this type of analysis is to answer questions such as

- What is the expected value of cogging torque, given distributions of critical manufacturing imperfections?
- What is the probability that a machine's cogging torque will exceed a certain value?
- What percentage of machines produced will satisfy a specific constraint on maximum cogging torque?
- What is the permissible tolerance of a specific feature, given a specific constraint on maximum cogging torque?

The approach taken here is to perform Monte Carlo simulations of the cogging torque. This entails generating a large set of random designs with each feature's level of deviation from the nominal design sampled according to a given probability density function (PDF). Each design is then evaluated using the analytical model. A histogram of the cogging torque can then be generated and from this, the PDF of the cogging torque can be derived. This approach is depicted in Fig. 5.

The method is not limited to the specific analytical model presented in this paper and can be implemented with any suitable analysis of the cogging torque that is capable of modeling the imperfections to be considered.

B. Case studies

In order to showcase the statistical modeling approach, case studies of the machines shown in Fig. 3 have been conducted. The nominal features of the designs are listed in Table II. Two hypothetical tolerance classes are considered. The standard deviations associated with each feature for the two tolerance classes are listed in Table V. In these case studies, it has been assumed that all machine features are normally distributed. However, the method can easily be implemented with different distributions for each feature.

For the case studies, the approach depicted in Fig. 5 has been implemented considering 10 000 samples in each

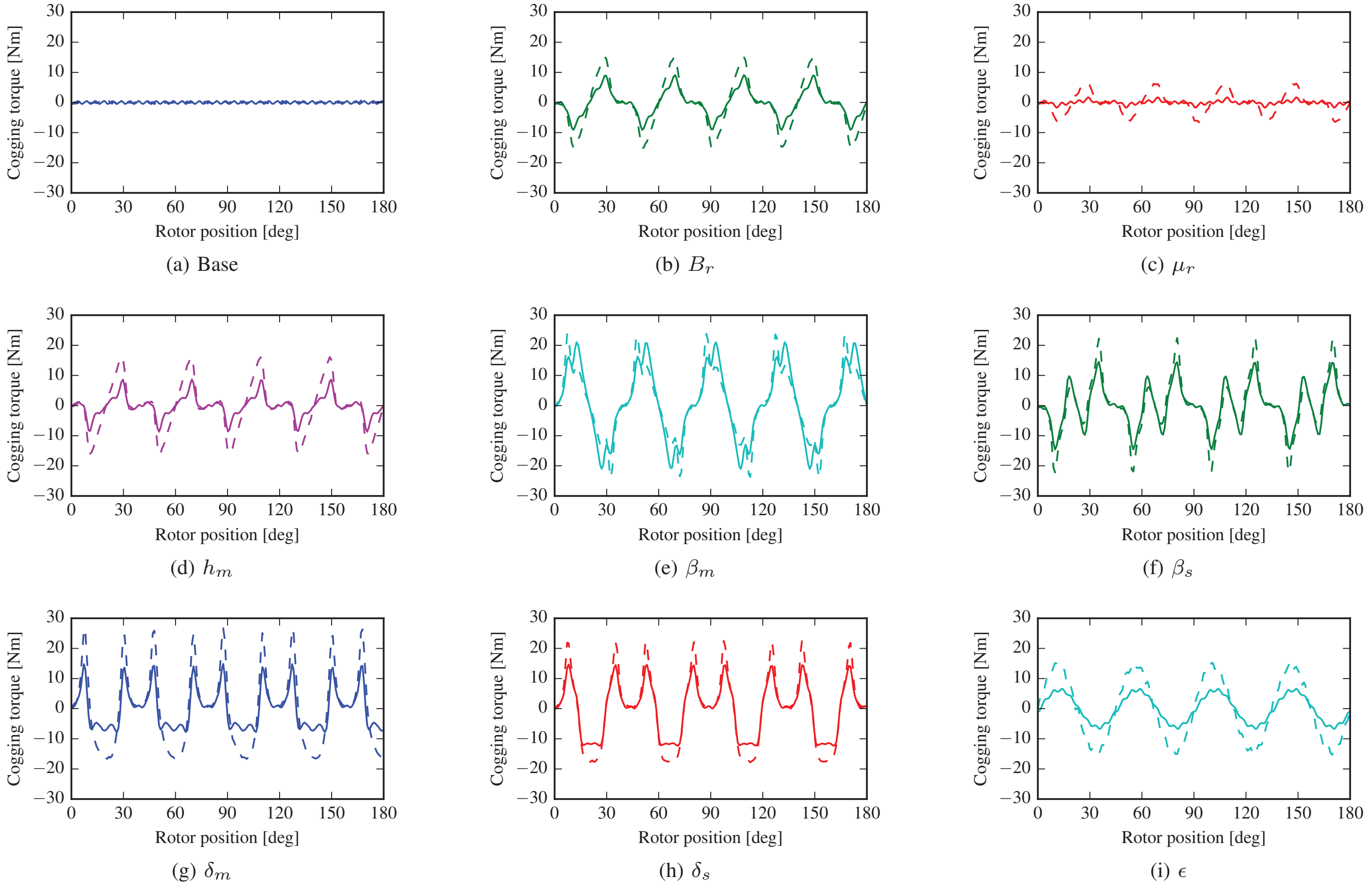

Fig. 4. Comparison of cogging torque waveforms for individual imperfections listed in Table IV.Solid line: Analytical model, dashed line: FEM.

case. The results for machines A and B are shown in Fig. 6. Besides the PDFs of the cogging torque, the nominal cogging torque (no imperfections) and the expected value of the cogging torque for both tolerance classes are also shown. In the case of machine A, it can be seen that manufacturing imperfections will cause the cogging torque of the vast of majority of machines to exceed the nominal value, although in a small number of cases, the cogging is lower than nominal. While the negative impact of wider tolerances is clear in Fig. 6a, the impact is much more severe in the case of machine B. Although the nominal cogging torque of machine B is very low, the design appears to be more sensitive to small imperfections. When manufacturing imperfections are introduced, virtually no machines will meet the nominal cogging torque specification.

In order to gain deeper insight into which imperfections have the greatest impact on the cogging torque, the correlation between specific imperfections and the cogging torque have been investigated. For this purpose, the magnitude of a specific imperfection for a sample has been calculated as

$$E^a = \frac{1}{N}\sum_{i=1}^{N} ||E_i|| \tag{19}$$

where E^a is the average error magnitude and E_i is the error of a specific feature, e.g. the deviation in the slot

TABLE V
FEATURE DISTRIBUTIONS

Feature	Standard deviation	
	Tight tolerances	Loose tolerances
B_r	0.01 T	0.02 T
μ_r	0.001	0.002
h_m	0.01 mm	0.02 mm
β_m	0.002	0.004
β_s	0.002	0.004
δ_m	0.4°	0.8°
δ_s	0.2°	0.4°
ϵ	40 μm	80 μm

opening of slot number i. The correlation between the various imperfections and the cogging torque for all four data sets are listed in Table VI. Based on this data, it seems that the tangential magnet and slot displacements δ_m and δ_s have the largest impact on the cogging torque. If these errors are eliminated, the cogging torque distributions of machines A and B with loose tolerances are shown in Fig. 7 and the expected values of the cogging torque is much closer to the nominal values.

C. Comparison with FEA results

A comparison of the histograms obtained using the analytical model and FEA for machine B with tight tolerances

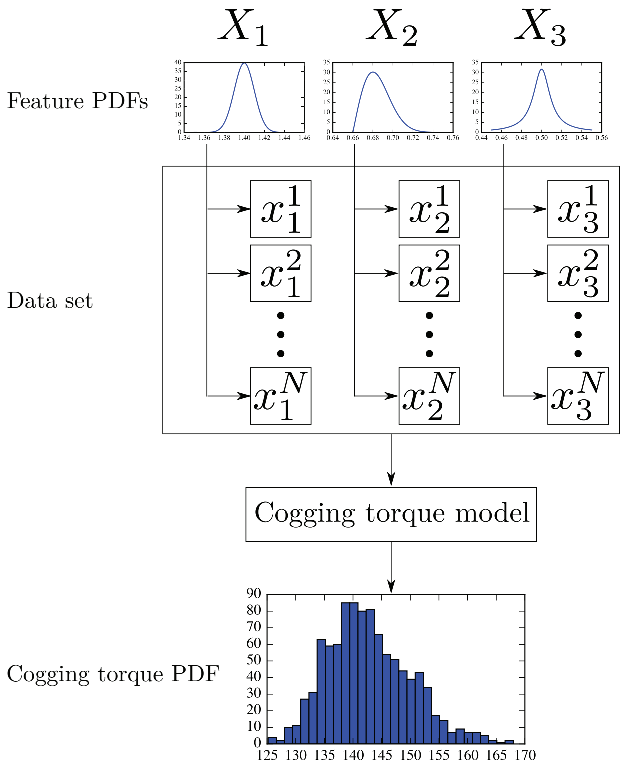

Fig. 5. Monte Carlo simulation approach employed to calculate a cogging torque probability density function.

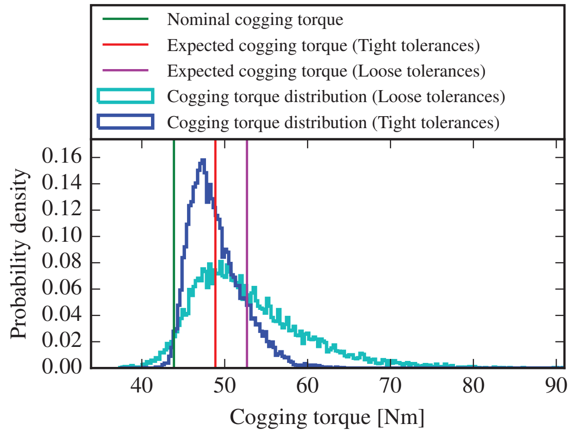

(a)

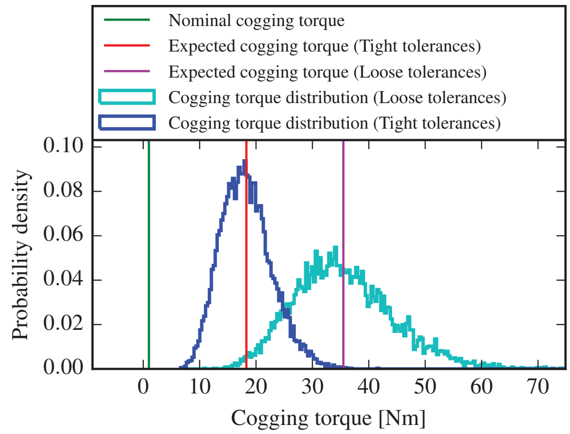

(b)

Fig. 6. Histograms of the cogging torque obtained for two hypothetical tolerance classes. (a) Machine A. (b) Machine B.

is shown in Fig. 8. These PDFs are not as smooth due to the reduced number of samples used for this comparison. The nominal values match closely, but there is a significant difference in the shape of the PDFs, with the FEA results showing a higher expected value. This comes as no surprise, considering that the analytical model tends to underestimate the impact of imperfections in this case, as is evident from Table IV and Fig. 4. Nevertheless, the analytical results give a reasonable indication of the impact that imperfections have on the cogging torque. The analytical results were generated in 45 seconds, while the finite element simulations took approximately 60 hours to complete.

V. Conclusions

This study has investigated the impact of manufacturing imperfections on the cogging torque of permanent magnet machines. An analytical model has been developed that is capable of accounting for several common manufacturing imperfections. A statistical approach to the analysis of cogging torque has been presented which considers the probability density distribution of machine features that have an impact on the cogging torque. The developed analytical model has been applied in examples of such statistical analyses. This approach allows a more realistic estimate of the expected cogging torque of machines produced in a mass production environment to be obtained.

While the presented analytical model may provide sufficient accuracy for certain topologies, modifications will be necessary if machines with alternative slot shapes and rotor topologies are to be modeled. Other analytical methods of calculating cogging torque, such as those based on complex permeance (conformal mapping) and subdomain models, can also be used. Although modeling intricate geometries with these methods is challenging, it is expected that improved accuracy can be achieved for a wider selection of rotor and stator geometries. Modeling imperfections with these methods is computationally more expensive than with the method presented in this paper. However, the cost is still expected to be far below that of using FEA such that statistical analyses, as presented in this paper, can be conducted within a reasonable amount of time.

References

[1] Z. Zhu and D. Howe, “Influence of Design Parameters on Cogging Torque in Permanent Magnet Machines,” *Energy Conversion, IEEE Transactions on*, vol. 15, no. 4, pp. 407–412, Dec. 2000.

[2] S.-M. Hwang, J.-B. Eom, Y.-H. Jung, D.-W. Lee and B.-S. Kang, “Various Design Techniques to Reduce Cogging Torque by Controlling Energy Variation in Permanent Magnet Motors,” *IEEE Transactions on Magnetics*, vol. 37, no. 4, pp. 2806–2809, Jul. 2001.

[3] N. Bianchi and S. Bolognani, “Design Techniques for Reducing the Cogging Torque in Surface-Mounted PM Motors,” *Industry Applications, IEEE Transactions on*, vol. 38, no. 5, pp. 1259–1265, Sep. 2002.

TABLE VI
CORRELATION BETWEEN AVERAGE ERRORS AND COGGING TORQUE

Error	Correlation coefficient			
	Machine A		Machine A	
	Tight	Loose	Tight	Loose
$E^a_{B_r}$	0.00	0.01	0.02	0.02
$E^a_{\mu_r}$	0.01	-0.00	0.02	0.01
$E^a_{h_m}$	-0.02	0.00	0.00	-0.02
$E^a_{\beta_m}$	0.01	-0.00	0.02	0.04
$E^a_{\beta_s}$	-0.01	0.01	0.01	0.00
$E^a_{\delta_m}$	0.30	0.26	0.52	0.51
$E^a_{\delta_s}$	0.10	0.12	0.33	0.32
E_ϵ	0.05	0.07	0.04	0.07

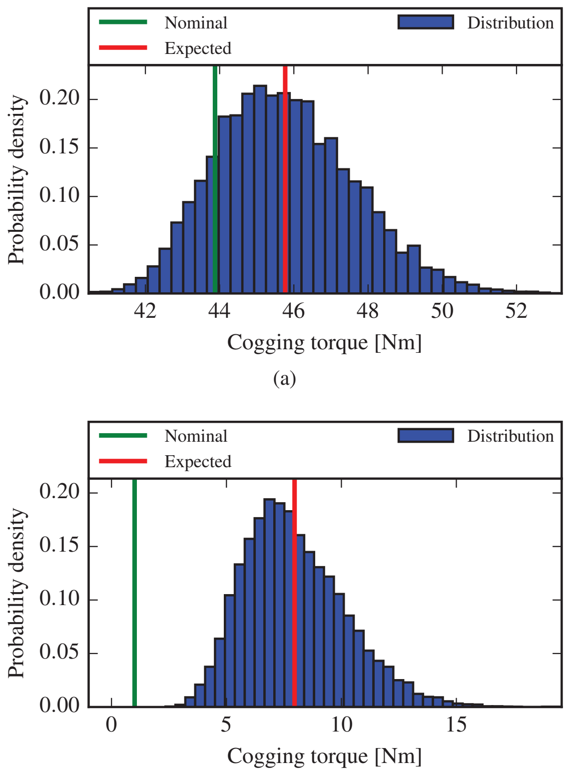

(a)

(b)

Fig. 7. Histograms considering loose tolerances and zero tangential displacement errors. (a) Machine A. (b) Machine B.

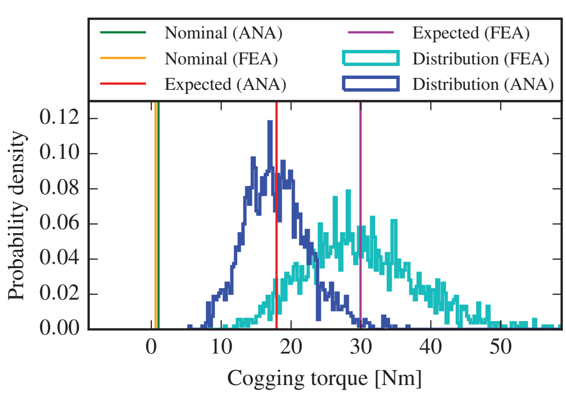

Fig. 8. Comparison of histograms obtained (2000 samples) using the analytical model (ANA) and FEA for cogging torque analyses.

[4] L. Dosiek and P. Pillay, "Cogging Torque Reduction in Permanent Magnet Machines," in *Industry Applications Conference, 41st IAS Annual Meeting*, vol. 1, Oct. 2006, pp. 44–49.

[5] L. Gasparin, A. Cernigoj, S. Markic and R. Fiser, "Additional Cogging Torque Components in Permanent-Magnet Motors Due to Manufacturing Imperfections," *IEEE Transactions on Magnetics*, vol. 45, no. 3, pp. 1210–1213, Mar. 2009.

[6] G. Heins, T. Brown and M. Thiele, "Statistical Analysis of the Effect of Magnet Placement on Cogging Torque in Fractional Pitch Permanent Magnet Motors," *IEEE Transactions on Magnetics*, vol. 47, no. 8, pp. 2142–2148, Aug. 2011.

[7] I. Coenen, M. van der Giet and K. Hameyer, "Manufacturing Tolerances: Estimation and Prediction of Cogging Torque Influenced by Magnetization Faults," *IEEE Transactions on Magnetics*, vol. 48, no. 5, pp. 1932–1936, May 2012.

[8] M. Khan, I. Husain, M. Islam and J. Klass, "Design of Experiments to Address Manufacturing Tolerances and Process Variations Influencing Cogging Torque and Back EMF in the Mass Production of the Permanent-Magnet Synchronous Motors," *Industry Applications, IEEE Transactions on*, vol. 50, no. 1, pp. 346–355, Jan. 2014.

[9] A. J. Pia, S. Paul, R. Islam and L. Xu, "Effect of Manufacturing Variations on Cogging Torque in Surface-Mounted Permanent Magnet Motors," in *Energy Conversion Congress and Exposition (ECCE)*, 2015.

[10] L. Zhu, S. Jiang, L. Zhu and C. Chan, "Comparison of Alternate Analytical Models for Predicting Cogging Torque in Surface-Mounted Permanent Magnet Machines," in *Vehicle Power and Propulsion Conference (VPPC)*, Sep. 2008, pp. 1–6.

[11] D. Zarko, D. Ban and T. Lipo, "Analytical Calculation of Magnetic Field Distribution in the Slotted Air Gap of a Surface Permanent-Magnet Motor Using Complex Relative Air-Gap Permeance," *IEEE Transactions on Magnetics*, vol. 42, no. 7, pp. 1828–1837, Jul. 2006.

[12] Z. Zhu, L. Wu and Z. Xia, "An Accurate Subdomain Model for Magnetic Field Computation in Slotted Surface-Mounted Permanent-Magnet Machines," *IEEE Transactions on Magnetics*, vol. 46, no. 4, pp. 1100–1115, Apr. 2010.

[13] L. Wu, Z. Zhu, D. Staton, M. Popescu and D. Hawkins, "Comparison of Analytical Models of Cogging Torque in Surface-Mounted PM Machines," *IEEE Transactions on Industrial Electronics*, vol. 59, no. 6, pp. 2414–2425, Jun. 2012.

[14] Z. Zhu and D. Howe, "Analytical Prediction of the Cogging Torque in Radial-Field Permanent Magnet Brushless Motors," *Magnetics, IEEE Transactions on*, vol. 28, no. 2, pp. 1371–1374, Mar. 1992.

[15] Z. Zhu, D. Howe, E. Bolte and B. Ackermann, "Instantaneous Magnetic Field Distribution in Brushless Permanent Magnet DC Motors. I. Open-Circuit Field," *IEEE Transactions on Magnetics*, vol. 29, no. 1, pp. 124–135, Jan. 1993.

[16] J. Gieras, "Analytical Approach to Cogging Torque Calculation of PM Brushless Motors," *Industry Applications, IEEE Transactions on*, vol. 40, no. 5, pp. 1310–1316, Sep. 2004.

Stiaan Gerber (M'13) was born in Bellville in South Africa on February 20, 1986. He received his PhD in Electrical Engineering at Stellenbosch University in 2015 where he is currently working as a postdoctoral researcher. His main interests in the engineering field are electrical machine design, numerical optimization, renewable energy power generation and finite element methods.

Rong-Jie Wang (M'00–SM'08) received the MSc(Eng) degree from the University of Cape Town in 1998 and the PhD(Eng) degree from Stellenbosch University in 2003, all of South Africa. He has been affiliated with the Department of Electrical and Electronic Engineering of Stellenbosch University since 2003, where he is currently an Associate Professor. His research interests include special electrical machines, computer-aided design and optimization of electrical machines, computational electromagnetics, thermal modeling of electrical machines and renewable energy systems. He has published more than 40 journal and conference papers and was a co-author of the monograph Axial Flux Permanent Magnet Brushless Machines (2nd ed., Springer 2008).